The Astrophysical Journal, 825:98 (10pp), 2016 July 10 doi:10.3847/0004-637X/825/2/98

WARM JUPITERS ARE LESS LONELY THAN HOT JUPITERS: CLOSE NEIGHBORS

Chelsea Huang[1,2], Yanqin Wu[3], and Amaury H. M. J. Triaud[1,3,4]
[1] Centre for Planetary Sciences, University of Toronto at Scarborough, 1265 Military Trail, Toronto, ON M1C 1A4, Canada; chelsea.huang@utoronto.ca
[2] Dunlap Institute, University of Toronto, Toronto, ON M5S 3H4, Canada
[3] Department of Astronomy & Astrophysics, University of Toronto, Toronto, ON M5S 3H4, Canada
[4] Institute of Astronomy, University of Cambridge, Madingley Road, Cambridge, CB3 0HA, UK
Received 2016 January 19; revised 2016 April 26; accepted 2016 April 27; published 2016 July 6

ABSTRACT

Exploiting the *Kepler* transit data, we uncover a dramatic distinction in the prevalence of sub-Jovian companions between systems that contain hot Jupiters (HJs) (periods inward of 10 days) and those that host warm Jupiters (WJs) (periods between 10 and 200 days). HJs, with the singular exception of WASP-47b, do not have any detectable inner or outer planetary companions (with periods inward of 50 days and sizes down to $2\,R_{\rm Earth}$). Restricting ourselves to inner companions, our limits reach down to $1\,R_{\rm Earth}$. In stark contrast, half of the WJs are closely flanked by small companions. Statistically, the companion fractions for hot and WJs are mutually exclusive, particularly in regard to inner companions. The high companion fraction of WJs also yields clues to their formation. The WJs that have close-by siblings should have low orbital eccentricities and low mutual inclinations. The orbital configurations of these systems are reminiscent of those of the low-mass close-in planetary systems abundantly discovered by the *Kepler* mission. This, and other arguments, lead us to propose that these WJs are formed in situ. There are indications that there may be a second population of WJs with different characteristics. In this picture, WASP-47b could be regarded as the extending tail of the in situ WJs into the HJ region and does not represent the generic formation route for HJs.

Key words: methods: statistical – planets and satellites: general

1. FOREWORDS

The origin of hot Jupiters (HJs, period inward of ∼10 days) has remained an unsolved issue. Although multiple scenarios have been proposed (disk migration, planet scattering, secular migration, etc.), none seem capable of satisfying all observational constraints. The recent discovery of two low-mass planetary companions (Becker et al. 2015) close to the HJ WASP-47b (Hellier et al. 2012) further obfuscates the picture. Motivated by the large population of low-mass, closely packed planets at small distances away from their host stars (Borucki et al. 2011; Lissauer et al. 2011; Mayor et al. 2011; Howard et al. 2012), and by the realization that some of them could have accumulated enough mass to undergo runaway gas accretion (Lee et al. 2014), Boley et al. (2016) and Batygin et al. (2015) argue that WASP-47b, and possibly all HJs, were formed in situ, instead of somehow transported inward. Only a tiny fraction of super-Earths need follow this path to be able to match the occurrence rate of HJs.

While this seems a reasonable proposal for WASP-47b, could it explain the majority of HJs? To answer this, we focus on the following issue: is WASP-47b a generic HJ in terms of cohabiting with other planets? Currently, this question is best addressed by exploiting the *Kepler* data to look for small transiting bodies in systems hosting (either confirmed or candidate) HJs. If we find that WASP-47b is truly unique among all HJs, it may suggest that the formation of HJs can have multiple pathways, with a minority being formed in situ.

There is a second goal to our paper: understanding the warm Jupiters (WJs). By this term we refer specifically to those giant planets orbiting between 10 and 200 days in period. Unlike the HJs (inward of 10 days), they are too far out to have experienced little if any tidal circularization and therefore may have difficulty migrating inward by mechanisms that invoke high-eccentricity excitation. On the other hand, they live inward of the sharp rise of giant planets outside ∼1 AU—in fact, the period range of WJs corresponds to the so-called "period-valley," the observed dip in occupation in between the HJs and cold Jupiters (e.g., Mayor et al. 2011; Wright et al. 2012; Santerne et al. 2016). In contrast with HJs, no theories have been proposed to explain the existence of this class of objects. So in this paper, we hope to gain some insights by studying their companion rates.

There have been multiple past claims that HJs lack sub-Jovian (and Jovian) close companions, by using the radial velocity (RV) data (Wright et al. 2009), by inferring from (the lack of) transit timing variations in these objects (Steffen & Agol 2005; Gibson et al. 2009; Latham et al. 2011; Steffen et al. 2012), and by searching for other transiting companions in the same systems (Steffen et al. 2012). The last study, in particular, is the closest to our work in spirit. Using preliminary candidates resulting from the first 4 months of the *Kepler* mission (63 HJs and 31 WJs, defined differently than here), Steffen et al. (2012) found a difference between the two populations: while none of the HJs have any transiting companions, 5 of the 31 WJ candidates do. These led them to suggest that HJs and WJs may be formed differently. However, due to the limitation of the short baseline of early-stage *Kepler* data and their crude criteria for candidate selection, their companion fractions are largely uncertain. For instance, among the five WJ candidates that were claimed to have companions, Kepler-18d, with a radius of $0.6\,R_J$, is actually a hot Neptune (Lithwick et al. 2012); KOI-190.01 is a diluted eclipsing binary (Santerne et al. 2012); and KOI-1300.01 is an eccentric eclipsing binary (Ofir & Dreizler 2013). This highlights the possible confusion that ensues when selecting candidates based on early *Kepler* light curves. Fortunately, 4 yr down the road, we not only have the full 4 yr *Kepler* data set at our disposal, but we also have a large number of confirmed Jovian planets to inform us on the

selection of candidates. We use both of these to our advantage and revisit the issue of companion fractions for close-in Jovian planets.

Our paper proceeds as follows. We first describe how we select our samples of hot and WJs from the *Kepler* data and how we evaluate our selection completeness in Section 2; the companion fractions of the two populations are estimated and presented in Section 2.3. We discuss the implications of our result on the formation paths of HJs and WJs in Section 3.

2. COMPANION FRACTIONS IN *KEPLER*

2.1. Sample Selection

We aim to construct a clean and complete giant-planet sample with a period range from 0.5 to 200 days from the full set of *Kepler* data. We select the planet candidates with a shorter-period range (0.5 to 34 days) from the *Kepler* Object of Interests (cumulative table) and then compensate the list of longer-period planets from existing literatures studying *Kepler* giant planets. We ensure a uniform selection of all candidates by making the same selection threshold as presented below on planet candidates from both origins.

We start with all the candidates with radii between 8 and 20 R_E. We then restrict ourselves to those around stars with more reliable stellar parameters in the *Kepler* Input Catalog (with stellar effective temperatures between 4500 and 6500 K). To reduce the false positive rate in the sample, we also require each of the planetary candidates to have a fitted impact parameter smaller than 0.9 and a fitted stellar density from transit parameters between 0.2 and 5 g cm^{-3} (Seager & Mallén-Ornelas 2003). We further remove candidates that have detectable secondary eclipses, or ellipsoidal variations, or centroid shifts during transit events.

The completeness and robustness of the *Kepler* candidates decrease for giant planets with longer orbital periods. A few teams released their own catalogs of long-period planetary candidates discovered within the *Kepler* data (Wang et al. 2013, i.e.,). In particular, Dawson et al. (2015) selected 31 KOIs with orbital periods longer than 34 days by using the combined catalog from all available sources (we refer to their Appendix A for their selection details).

We include the 22 candidates from Dawson et al. (2015) that have orbital periods between 34 and 200 days to complement our above selection, but reject five planetary candidates from that sample because of their V-shaped transits and/or anomalously large radius (also see the "exceptional candidate treatment" section of Dawson et al. 2015). These WJs matched our selection criterion for the KOIs with shorter orbital periods. Therefore, combining both samples preserves a uniform selection. We refer to our sample as the *Kepler* giant-planet sample in the text hereafter and do not specifically distinguish in the text between the concept of "planets" and "planet candidates."

We present our final sample in Tables 3 and 4. This sample includes all of the 40 confirmed giant planets from the catalog summarized by Santerne et al. (2016) matching our designed planet period and stellar property range. With our definitions of HJs and WJs, our sample includes 45 HJs (28 confirmed) and 27 WJs (12 confirmed). It does not, however, include the HJ WASP-47b, since it is not observed by the *Kepler* main mission.

In Figure 1, we compare the sizes of these objects with known Jupiters, as a function of their incident irradiations.

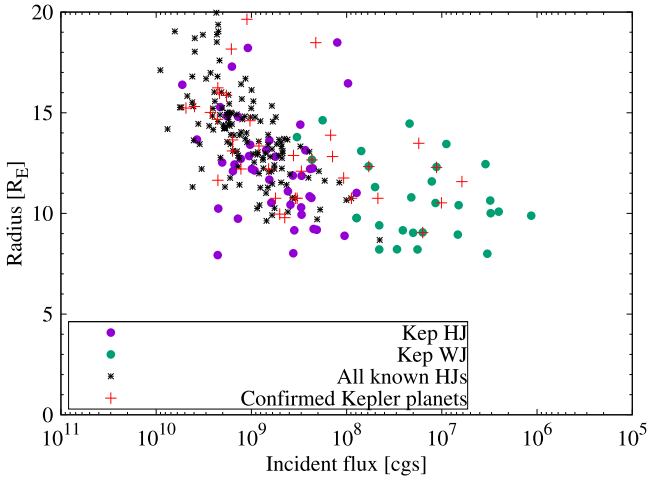

Figure 1. Radius of our selected planets vs. the incident irradiations they receive, compared with all of the known transiting HJs (black asterisks) and confirmed *Kepler* giant planets (red crosses). We separated our sample into two groups: the HJs ($P < 10$ days) are shown with purple dots, and the ones with longer orbital periods (WJs) are shown with green dots.

They appear to fall into a similar region, suggesting that the fraction of false positives in our sample is small. More quantitatively, Morton (2012) developed a statistical framework to quantify false positive probabilities of *Kepler* candidates. Judging by his values for the unconfirmed objects in our sample (Tables 3 and 4), the majority have negligible probabilities to be false positives.

2.2. Search and Completeness of Small-sized Planets

We seek additional companions in systems hosting our selection of giant planets. To address the possibility that the giant-planet transit signals would influence the detrending process and the transit search algorithm, we first removed all of their transits from the *Kepler* raw (simple aperture, SAP) light curves. For each expected giant-planet transit, this is done by creating a data gap in the light curve with a width 1.1× the fitted transit duration and centered on the transit epoch. We then detrended the light curves following Huang et al. (2013) and searched for additional transit signals using a box-fitting least-squares (BLS) algorithm. Any BLS peaks detected with transit dip significances (signal-to-noise ratio [S/N] of the transit signal) higher than 10 are investigated to check whether they are due to planet signals.

Moreover, we can also calculate the completeness of detection for a planet of a given size and at a given period, based on the estimated S/N,

$$\mathrm{S/N} = \frac{\delta}{\mathrm{CDPP}} \times \sqrt{N_{\mathrm{transit}}}\,. \quad (1)$$

Here δ is the expected transit depth for the planet, N_{transit} the number of transits in the entire *Kepler* light curve, and CDPP the combined differential photometric precision of the light curve over the transit duration timescale. Fressin et al. (2013) reported that 99.9% of the *Kepler* candidates with an S/N larger than 10.1 will be detected by the *Kepler* pipeline. When calculating the completeness, we define a planet as detectable if its S/N is greater than 10. A histogram of the 6.5 hr CDPP values for host stars in our sample is shown in Figure 2. The host stars of HJs and WJs have similar noise properties in their

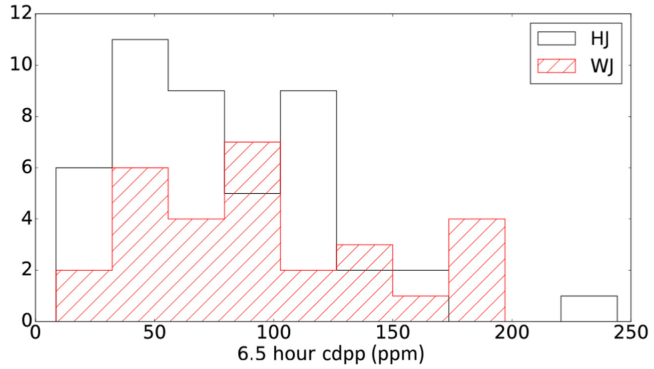

Figure 2. Histogram of the 6.5 hr CDPP for the light curves of the host stars in our *Kepler* giant-planet sample. Those with HJs are shown in black, while those with WJs are shown in red. The two populations have similar noise properties.

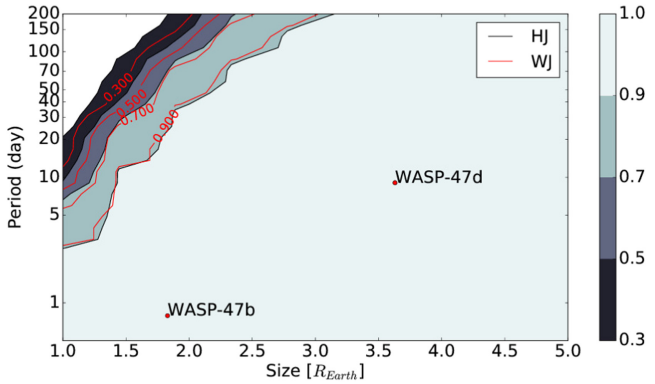

Figure 3. Detection completeness as a function of planet size (in Earth radii) and orbital period (in days) for our systems. The contours (and black lines) show the averaged completeness of all HJ systems, while the red lines show that for the WJ systems. They are similar. For planets larger than 2 $R_{\rm Earth}$, we are >90% complete out to 50 days, while for those larger than 1 $R_{\rm Earth}$, we are >90% complete out to ~3 days. The latter places a stringent constraint on the inner companions of HJs. The interior and exterior companions of WASP-47c are noted here. They are trivially detectable around all systems.

light curves. So we expect similar detection completeness in these two groups.

We report the detection completeness thus estimated in Figure 3, averaged over the cohorts of HJ and WJ systems separately. As expected, they look rather similar. We further verify this estimation by performing a signal-injection-and-recovery experiment. We inject into the HJ light curves transit signals by planets of orbital period around 10 days and of various sizes (2 $R_{\rm Earth}$, 1.5 $R_{\rm Earth}$, and 1 $R_{\rm Earth}$). We obtain recovery rates of 100%, 93%, and 51% at these sizes. These match the above estimates using light-curve CDPPs.

Also shown in Figure 3 are the positions of the two small companions of WASP-47b. If present, they should be trivially detected around any of the giant planets in our sample.

2.3. Results

We summarize our search results in Table 1. We find that while none of the HJs have any transiting companions, 11 (out of 27) of the WJs do. All of these companions have also been reported by the *Kepler* candidate catalog. We display the orbit architectures of these multiple systems in Figures 4 and 5.

Assuming that all companions to the giant planets transit, we can estimate simply the companion fractions using results in Table 1. We focus on companions inward of 50 days and larger than 2 $R_{\rm Earth}$, since this population should be detected nearly completely (>90%), and since most of the companions we find do fall in this range. We call these "close" companions. We treat the problem as an estimation of the distribution of the event success rate p for a binomial distribution having observed s successes in n trials, for which each system is assumed to have equal weight. We imply a conjugate prior (Beta(0.5, 0.5)) on p. The posterior distribution of p can be expressed as Beta(s + 0.5, $n - s$ + 0.5). We thereby obtain a multiplicity rate of HJs of $0.52^{+5.0}_{-0.52}$%, while that for WJs is $37.2^{+18.6}_{-16.3}$%. Throughout this work, we present results in terms of the median of the distribution and their 90% confidence interval.

If we only use the confirmed planet systems, the estimated multiplicity rate for HJs is Beta(0.5, 28.5) = $0.8^{+7.7}_{-0.8}$% and for WJs is Beta(8.5, 4.5) = $58.1^{+23.9}_{-26.9}$. The latter value, however, should be taken with caution as the confirmed systems are likely to bias toward multiple systems. As an example, they are usually prioritized during RV follow-up observations. Other confirmation methods, such as transit timing variation (Xie 2013, i.e.,), or making use of low false positive rates of the *Kepler* multiple systems (Rowe et al. 2014, i.e.,), also prefer to confirm multiple systems.

2.3.1. Monte Carlo Simulation

To have a more realistic estimation that takes into account a multitude of observational uncertainties, we perform a Markov chain Monte Carlo simulation with emcee (Foreman-Mackey et al. 2013) to constrain the rate of multiplicity.

For our standard MCMC model, we again assume that all companions transit (a flat system), and we adopt a false positive rate of 50% for the unconfirmed planets in our sample. We continue to focus on "close" companions for which our detection capacity is nearly complete. We also account for the scatter of the Neptune population into our sample. The details are laid out in the Appendix, and the results are shown in the top panel of Figure 6. We obtain that HJs have a multiplicity rate of $1.1^{+13.3}_{-1.1}$% and WJs have a multiplicity rate of $55.7^{+27.0}_{-31.1}$%, largely unchanged from our previous estimates.

In the following, we relax or alter some of the assumptions in our standard model. Results of all these experiments are summarized in Table 2.

2.3.2. Impact of False Positives

Figure 6 compares the results when different false positive rates for the unconfirmed systems are adopted. The overall effect of a smaller false positive rate is to reduce the companion fraction for WJs, since the confirmed WJs have a higher multiplicity than the unconfirmed ones.

We note that the false positive rate we adopt for our standard model (fp = 50%) is likely too pessimistic for our sample. This value is derived by Santerne et al. (2016) for all giant candidates in the entire *Kepler* candidate sample, while we benefit from additional filtering based on follow-up measurements and additional vetting on the light curves. In fact, the individualized false positive rates (Morton et al. 2016, in preparation) for the unconfirmed objects in our sample are in general low. We regard an optimistic value of fp = 10% as calculated from the above work to be more suitable for our WJ candidates. We will present more results for this false positive rate below.

Table 1
Kepler Hot Jupiter Systems

KIC	Period (day)	R_p ($R_{\rm Earth}$)	M_p ($M_{\rm Jup}$)	$R_{\rm star}$ ($R_\odot$)	*fp* Rate[a]	Other Name/Reference[b]
9115800	4.454194338	$12.21^{+7.19}_{-1.6}$	n/a	$0.915^{+0.539}_{-0.12}$	6.5×10^{-5}	KOI-421.01
8544996	4.082275068	$10.85^{+4.31}_{-0.81}$	n/a	$0.707^{+0.316}_{-0.06}$	2.1×10^{-6}	KOI-913.01
7832356	7.886631104	$9.23^{+3.33}_{-1.62}$	n/a	$1.135^{+0.409}_{-0.199}$	1.3×10^{-11}	KOI-1456.01
4076098	3.990106229	$8.02^{+3}_{-0.69}$	n/a	$0.9130^{+0.341}_{-0.079}$	9×10^{-5}	KOI1323.01
9643874	8.027680595	$8.89^{+3.39}_{-0.63}$	n/a	$0.887^{+0.338}_{-0.063}$	1.1×10^{-3}	KOI1457.01
7585481	8.098887986	$9.19^{+4.66}_{-0.85}$	n/a	$1.064^{+0.54}_{-0.098}$	8.4×10^{-9}	KOI890.01
3351888	1.625522200	$9.74^{+3.88}_{-1.24}$	n/a	$1.057^{+0.421}_{-0.135}$	5.8×10^{-7}	KOI801.01
9141746	6.491684259	$10.30^{+6.12}_{-1.24}$	n/a	$1.13^{+0.67}_{-0.14}$	3.2×10^{-4}	KOI-929.01
8255887	4.708326542	$11.10^{+4.17}_{-2.41}$	n/a	$1.21^{+0.46}_{-0.26}$	4.9×10^{-5}	KOI908.01
11138155	4.959319451	$11.88^{+4.91}_{-1.08}$	n/a	$1.025^{+0.424}_{-0.093}$	1.7×10^{-2}	KOI-760.01
10019708	3.268695154	$12.13^{+7.48}_{-1.4}$	n/a	$1.171^{+0.722}_{-0.135}$	1.3×10^{-10}	KOI-199.01
11414511	2.816504852	$12.82^{+4.94}_{-1.39}$	n/a	$0.9650^{+0.371}_{-0.105}$	5.8×10^{-4}	KOI-767.01
9595827	3.905081985	$13.14^{+0.86}_{-0.49}$	n/a	$0.8870^{+0.058}_{-0.033}$	8.1×10^{-4}	KOI-217.01
12019440	3.243259796	$13.63^{+6.16}_{-1.23}$	n/a	$1.0290^{+0.465}_{-0.299}$	1.7×10^{-3}	KOI-186.01
8323764	6.714251076	$16.46^{+6.05}_{-1.79}$	n/a	$0.8^{+0.29}_{-0.084}$	3.4×10^{-2}	KOI-3767.01
6849046	4.225384512	$9.00^{+1.76}_{-0.66}$	n/a	$1.05^{+0.21}_{-0.08}$	0	KOI-201.01 (Sa12)
7778437	5.014234575	$10.31^{+7.57}_{-1.54}$	n/a	$1.31^{+0.26}_{-0.26}$	0	KOI131.01 (Sa12)
7017372	5.240904530	$12.84^{+6.69}_{-2.52}$	n/a	$1.41^{+0.59}_{-0.24}$	0	KOI-3689.01 (Sa12)
757450	8.884922680	$11.30^{+0.66}_{-0.66}$	$9.9^{+0.5}_{-0.5}$	$0.88^{+0.04}_{-0.04}$	0	Kepler-75b (Bo15)
4570949	1.544928883	$14.92^{+1.32}_{-1.32}$	$2.01^{+0.37}_{-0.35}$	$1.32^{+0.08}_{-0.08}$	0	Kepler-76b (Fa13)
5357901	3.797018335	$10.73^{+0.24}_{-0.24}$	$0.25^{+0.08}_{-0.08}$	$0.86^{+0.02}_{-0.02}$	0	Kepler-425b (He14)
5358624	3.525632561	$11.85^{+0.33}_{-0.33}$	$1.27^{+0.19}_{-0.19}$	$0.80^{+0.02}_{-0.02}$	0	Kepler-428b (He14)
5728139	5.334083460	$15.91^{+1.76}_{-1.76}$	$2.82^{+0.52}_{-0.52}$	$2.26^{+0.25}_{-0.25}$	0	Kepler-433b (Al12)
5780885	4.885488953	$17.78^{+0.11}_{-0.11}$	$0.44^{+0.04}_{-0.04}$	$1.96^{+0.07}_{-0.07}$	0	Kepler-7b (La10)
6046540	7.340714746	$10.53^{+0.22}_{-0.22}$	$0.63^{+0.12}_{-0.12}$	$1.12^{+0.04}_{-0.04}$	0	Kepler-74b (Bo15)
6922244	3.522498573	$15.58^{+0.55}_{-0.66}$	$0.59^{+0.13}_{-0.12}$	$1.45^{+0.12}_{-0.13}$	0	Kepler-8b (Je10)
7529266	8.600153301	$21.84^{+1.98}_{-1.98}$	$0.84^{+0.15}_{-0.15}$	$3.21^{+0.3}_{-0.3}$	0	Kepler-435b (Al12)
7877496	1.720861324	$14.70^{+0.44}_{-0.55}$	$0.94^{+0.12}_{-0.02}$	$1.29^{+0.04}_{-0.04}$	0	Kepler-412b (De14)
8191672	3.548465405	$15.69^{+0.44}_{-0.55}$	$2.11^{+0.07}_{-0.09}$	$1.75^{+0.14}_{-0.15}$	0	Kepler-5b (Ko10)
9305831	3.246732651	$11.96^{+0.77}_{-0.77}$	$1.00^{+0.1}_{-0.1}$	$1.35^{+0.08}_{-0.08}$	0	Kepler-44b (Bo12)
9410930	1.855557540	$11.41^{+0.44}_{-0.44}$	$0.56^{+0.10}_{-0.09}$	$1.02^{+0.03}_{-0.03}$	0	Kepler-41b (Es15)
9631995	7.891448474	$12.62^{+1.21}_{-1.21}$	$0.43^{+0.13}_{-0.13}$	$1.24^{+0.12}_{-0.12}$	0	Kepler- 422b (En14)
9651668	2.684328485	$13.17^{+0.77}_{-0.77}$	$0.72^{+0.12}_{-0.12}$	$0.99^{+0.05}_{-0.05}$	0	Kepler-423b (En14)
9818381	3.024092548	$13.39^{+0.77}_{-0.66}$	$3.23^{+0.26}_{-0.26}$	$1.38^{+0.05}_{-0.03}$	0	Kepler-43b (Es15; Bo15)
10264660	6.790121599	$12.46^{+0.59}_{-0.59}$	$8.4^{+0.19}_{-0.19}$	$2.05^{+0.08}_{-0.08}$	0	Kepler-14b (Bu11)
10619192	1.485710952	$14.59^{+0.44}_{-0.44}$	$2.47^{+0.10}_{-0.10}$	$1.17^{+0.09}_{-0.09}$	0	Kepler-17b (Bo12)
10666592	2.204735365	$15.69^{+1.2}_{-1.2}$	$1.741^{+0.028}_{-0.028}$	$2.00^{+0.01}_{-0.02}$	0	HAT-P-7b (Pa08; Va13)
10874614	3.234699312	$14.26^{+0.22}_{-0.33}$	$0.67^{+0.04}_{-0.04}$	$1.29^{+0.09}_{-0.10}$	0	Kepler-6b (Es15)
11017901	7.794301316	$18.10^{+6.47}_{-6.47}$	$1.37^{+0.48}_{-0.48}$	$1.03^{+0.16}_{-0.16}$	0	Kepler-447b (Li15)
11359879	4.942783399	$10.54^{+0.66}_{-0.77}$	$0.66^{+0.08}_{-0.09}$	$0.98^{+0.16}_{-0.06}$	0	Kepler-15b (En11)
11804465	4.437963030	$19.20^{+0.33}_{-0.44}$	$0.43^{+0.05}_{-0.05}$	$1.42^{+0.30}_{-0.24}$	0	Kepler-12b (Es15)
11446443	2.4706133738	$13.05^{+0.27}_{-0.27}$	$1.253^{+0.052}_{-0.052}$	$1.0^{+0.036}_{-0.036}$	0	Tres-2b (Od06; So10)
11502867	3.217518593	$11.96^{+0.33}_{-0.33}$	$0.34^{+0.08}_{-0.08}$	$0.92^{+0.02}_{-0.02}$	0	Kepler-426b (He14)
9941662	1.763587569	$16.57^{+0.44}_{-0.44}$	$9.28^{+0.16}_{-0.16}$	$1.74^{+0.04}_{-0.04}$	0	Kepler-13b (Sh11)
8359498	3.578780551	$10.53^{+0.22}_{-0.22}$	$0.43^{+0.03}_{-0.03}$	$0.99^{+0.02}_{-0.02}$	0	KOI127.01 (Ga13)

Notes.
[a] False positive rate for individual system *fp* is from the NASA Exoplanet Archive *Kepler* false positive probability table based on Morton et al. (2016, in preparation). See http://exoplanetarchive.ipac.caltech.edu/cgi-bin/TblView/nph-tblView?app=ExoTbls&config=koifpp. We assign 0 to the confirmed candidates.
[b] Reference abbreviations used in this table and the next are as follows. Al12: Almenara et al. (2015); Bo12: Bonomo et al. (2012); Bo15: Bonomo et al. (2015); Br15: Bruno et al. (2015); Bu11: Buchhave et al. (2011); Ca14: Cabrera et al. (2014); Da12: Dawson et al. (2012); De14: Deleuil et al. (2014); En11: Endl et al. (2011); En14: Endl et al. (2014); Es15: Esteves et al. (2015); Fa13: Faigler et al. (2013); Ga13: Gandolfi et al. (2013); He14: Hébrard et al. (2014); Je10: Jenkins et al. (2010); Ko10: Koch et al. (2010); La10: Latham et al. (2010); Li15: Lillo-Box et al. (2014); Ne12: Nesvorný et al. (2012); Od06: O'Donovan et al. (2006); Pa08: Pál et al. (2008); Sa12: Sanchis-Ojeda et al. (2012); Sa12: Santerne et al. (2012); Sa12: Santerne et al. (2016); Sc14: Schmitt et al. (2014b); Sc14b: Schmitt et al. (2014a); Sh11: Shporer et al. (2011); St10: Steffen et al. (2010); So10: Southworth (2011); Ro14: Rowe et al. (2014); Va13: Van Eylen et al. (2012); We13: Weiss et al. (2013).

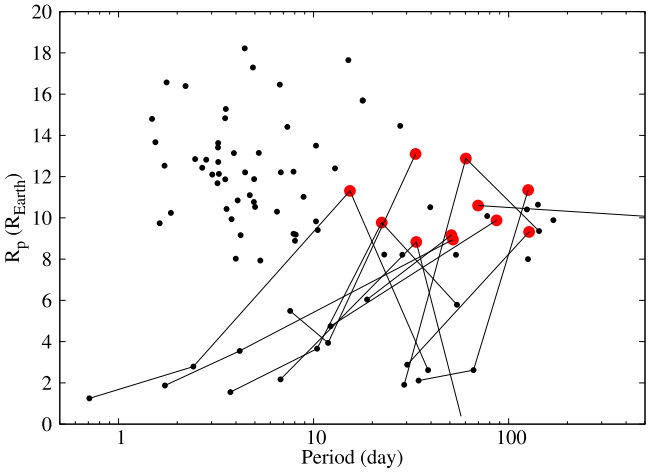

Figure 4. Periods and radii for our sample of giant planets and their neighbors. The giant planets that have companions are marked out in red and are connected to their companions by lines. Only WJs appear to belong to multiple systems.

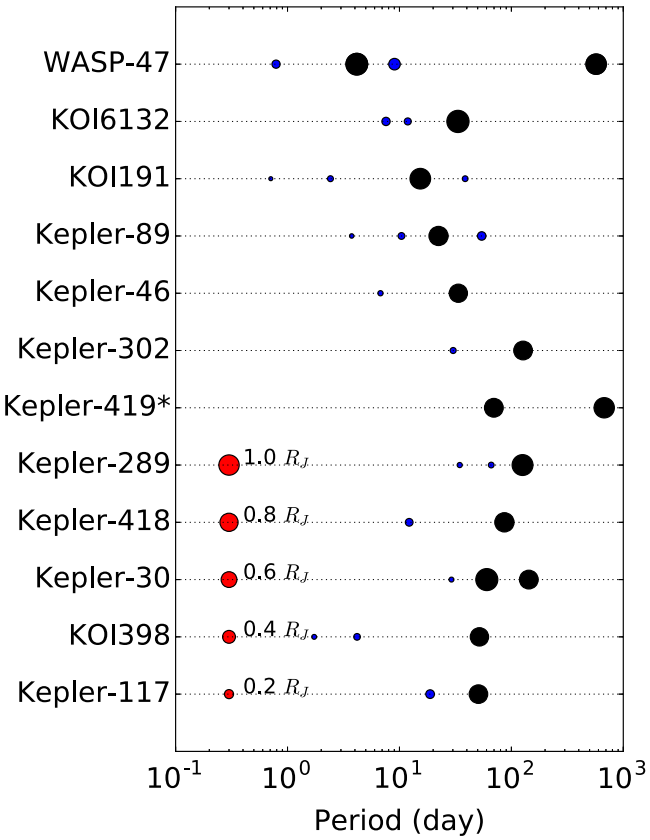

Figure 5. Similar to Figure 4, but showing more clearly the architectures of our multiple systems (around WJs). The planets are laid out in log P, with the size of the dot representing the size of the planet. The confirmed systems are noted by their *Kepler* names. The Kepler-419 system is counted as a single WJ system in our calculation, given that the companion is far away.

2.3.3. Impact of Mutual Inclination

So far, we have assumed that the companions always transit. Fabrycky et al. (2014) found that the *Kepler* multiple systems are indeed quite coplanar (also see Fang & Margot 2012; Figueira et al. 2012; Tremaine & Dong 2012). Assuming that the mutual inclination (μ) dispersion follows a Rayleigh distribution, the inferred dispersion σ_μ typically lies in the range 1°.0–2°.2. We investigate how this affects our results.

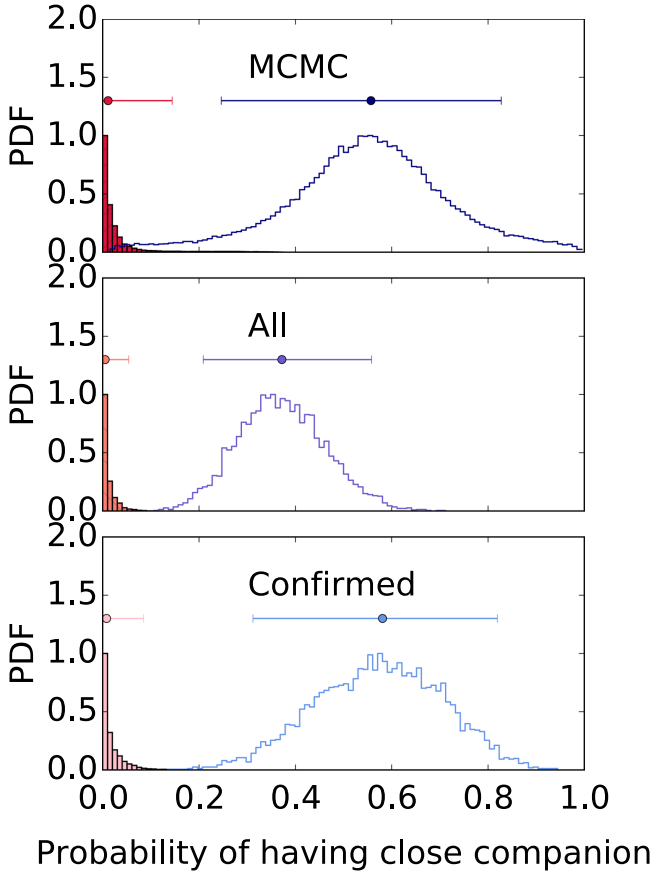

Figure 6. Probability density distributions for giant planets to have "close" companions, defined as inward of 50 days and larger than 2 R_{Earth}. Here, we assume that all planets in a given system transit. The top panel compares the companion rates for HJs (blue) and WJs (red) in our standard Monte Carlo model, where the candidate false positive rate is assumed to be 50%. Points with error bars indicate the median of the distribution and its 90% confidence interval. The middle panel assumes that all unconfirmed candidates are real planets ($fp = 0$), whereas the bottom panel assumes that they are all false positives ($fp = 100\%$), and only confirmed planets are included. The two populations of giant planets are incompatible in all cases.

We consider only the possibility that the giant-planet systems have a nontransiting companion interior to the giant planet. As the transit probability is now a function of orbital period, we need to assume a period distribution for the companion. The occurrence rate of sub-Jovian planets is roughly flat in the log period space and falls off for short periods (Howard et al. 2012; Dong & Zhu 2013). We assume that the companion occurrence rate is flat in log P for WJs, with an inner cutoff period of 1 day, and a period power-law dependence for period for HJs, with an inner cutoff period of 0.5 days. We simulate the rate of an interior companion assuming that the prior for the mutual inclination follows a Rayleigh distribution with $\sigma_\mu = 1°.8$ for both the HJs and WJs. To explore the extremes, we also simulate the rate of the interior companion for HJs assuming that the cos μ distribution is uniform between 0 and 1. The distribution of the interior companion rate is constrained as in the top panel of Figure 7, using a false positive rate of 50%. We show that, assuming the same mutual inclination distribution, the medians of the multiplicity rate distributions of HJs and WJs both shift to a

Table 2
Kepler Warm Jupiter Systems

KIC	Period (days)	R_p ($R_{\rm Earth}$)	M_p ($M_{\rm Jup}$)	$R_{\rm star}$ ($R_\odot$)	*fp* rate	Other Name/Reference
7984047	77.63425713	$10.09^{+1.35}_{-0.91}$	n/a	$0.755^{+0.101}_{-0.068}$	8.8×10^{-3}	KOI-1552.01
7811397	169.49954	$9.89^{+2.26}_{-0.81}$	n/a	$0.719^{+0.164}_{-0.059}$	0.71	KOI-1477.01
8672910	39.64317811	$10.52^{+4.46}_{-0.81}$	n/a	$0.833^{+0.355}_{-0.064}$	3.6×10^{-4}	KOI-918.01
7504328	53.71797107	$8.21^{+2.73}_{-1.59}$	n/a	$1.151^{+0.383}_{-0.222}$	0.46	KOI-458.01
6471021	125.62887621	$8^{+1.14}_{-0.34}$	n/a	$0.897^{+0.128}_{-0.038}$	2.2×10^{-4}	KOI-372.01
6061119	27.807562927	$14.46^{+6.63}_{-1.08}$	n/a	$0.791^{+0.363}_{-0.059}$	7.7×10^{-2}	KOI-846.01
4760746	15.068059056	$17.65^{+5.88}_{-1.64}$	n/a	$0.96^{+0.32}_{-0.089}$	0.8	KOI-1455.01
10656508	124.03590546	$10.41^{+6.91}_{-1.14}$	n/a	$1.137^{+0.754}_{-0.125}$	7.9×10^{-3}	KOI-211.01
7950644	10.290993755	13.776 ± 2.35	0.29 ± 0.09	1.35 ± 0.2	0	Kepler-427b (He14)
4164994	10.506825646	$9.41^{+1.89}_{-0.64}$	n/a	$0.784^{+0.157}_{-0.054}$	7.5×10^{-4}	KOI-1320.01
11194032	28.511205250	$8.21^{+6.23}_{-4.56}$	n/a	$1.741^{+1.322}_{-0.966}$	0	KOI-348.01
7499398	23.020303180	$8.22^{+3.19}_{-0.68}$	n/a	$0.95^{+0.368}_{-0.079}$	9.4×10^{-3}	KOI-1473.01
7368664	12.874711418	$12.40^{+2.85}_{-1.98}$	$2.86^{+0.35}_{-0.35}$	$1.38^{+0.13}_{-0.13}$	0	Kepler-434b (Al12)
7951018	52.75875577	$9.04^{+5.84}_{-1.04}$	n/a	$1.154^{+0.746}_{-0.132}$	8.5×10^{-4}	KOI-1553.01
9025971	141.24164672	$10.64^{+4.02}_{-0.85}$	$0.55^{+0.02}_{-0.02}$	$0.913^{+0.345}_{-0.073}$	0	KOI-3680.01 (Sa12)
5812701	17.855219698	$15.69^{+1.43}_{-1.43}$	n/a	$1.63^{+0.15}_{-0.15}$	0	KOI-12.01 (Bo15)
10723750	50.79034619	$9.16^{+5.55}_{-1.14}$	$1.84^{+0.18}_{-0.183}$	$1.183^{+0.716}_{-0.147}$	0	Kepler-117c (Ro14; Br15)
	18.795900480	$6.04^{+3.66}_{-0.75}$	$0.094^{+0.03}_{-0.03}$	⋯	0	Kepler-117b (Ro14; Br15)
7109675	33.601220660	$8.83^{+0.46}_{-0.5}$	n/a	$0.93^{+0.048}_{-0.053}$	0	Kepler-46b (Ne12)
	57.011	n/a	$0.376^{+0.021}_{-0.019}$	⋯	0	Kepler-46c (Ne12)
	6.76652078	$2.17^{+0.11}_{-0.13}$	n/a	⋯	0	Kepler-46d (Ne12)
6462863	22.342969585	$9.77^{+2.03}_{-1.5}$	$0.333^{+0.036}_{-0.036}$	$1.297^{+0.27}_{-0.199}$	0	Kepler-89d (We13)
	10.423677765	$3.66^{+0.76}_{-0.56}$	0.030 ± 0.015	⋯	0	Kepler-89c (We13)
	54.31998605	$5.79^{+1.21}_{-0.89}$	0.1101 ± 0.045	⋯	0	Kepler-89e (We13)
	3.743175556	$1.55^{+0.32}_{-0.24}$	0.02 ± 0.02	⋯	0	Kepler-89b (We13)
5972334	15.358768403	$11.31^{+4.78}_{-1.04}$	n/a	$0.87^{+0.368}_{-0.08}$	4.1×10^{-4}	KOI-191.01 (St10)
	2.418405445	$2.79^{+1.17}_{-0.26}$	n/a	⋯	3×10^{-3}	KOI-191.02 (St10)
	0.708620008	$1.25^{+0.52}_{-0.12}$	n/a	⋯	1.0	KOI-191.03 (St10)
	38.6519976	$2.62^{+1.11}_{-0.24}$	n/a	⋯	1.3×10^{-3}	KOI-191.04 (St10)
5629353	33.319916700	$13.10^{+7.22}_{-3.66}$	n/a	$1.63^{+0.897}_{-0.456}$	2×10^{-2}	KOI-6132.01
	7.5844126	$5.49^{+3.03}_{-1.53}$	n/a	⋯	3.8×10^{-4}	KOI-6132.02
	11.8674823	$3.94^{+2.17}_{-1.1}$	n/a	⋯	3.7×10^{-3}	KOI-6132.03
9946525	51.84688575	$8.95^{+2.07}_{-0.65}$	n/a	$0.838^{+0.252}_{-0.061}$	4.43-3	KOI-398.01
	4.18004955	$3.55^{+1.07}_{-0.26}$	n/a	⋯	3.8×10^{-7}	Kepler-148c
	1.729366467	$1.87^{+0.56}_{-0.15}$	n/a	⋯	0.88	Kepler-148b
3832474	143.2063518	$9.36^{+0.99}_{-0.37}$	$0.073^{+0.008}_{-0.008}$	$0.867^{+0.092}_{-0.034}$	0	Kepler-30d (Sa12)
	60.32488611	$12.88^{+1.36}_{-0.51}$	$2.01^{+0.16}_{-0.16}$	⋯	0	Kepler-30c (Sa12)
	29.1598615	$1.91^{+0.2}_{-0.07}$	$0.036^{+0.004}_{-0.004}$	⋯	0	Kepler-30b (Sa12)
3247268	86.67855186	$9.88^{+4.67}_{-1.02}$	$1.1^{+1.1}_{-0.0}$	$1.043^{+0.494}_{-0.107}$	0	Kepler- 418b
	12.218278	$4.75^{+2.25}_{-0.49}$	n/a	⋯	2.0×10^{-4}	KOI-1089.02
7303287	125.8518	$11.35^{+0.19}_{-0.19}$	$0.41^{+0.05}_{-0.05}$	$1.00^{+0.02}_{-0.02}$	0	Kepler-289b (Sc14b)
	34.5438464	$2.11^{+0.1}_{-0.1}$	n/a	⋯	0	Kepler-289c (Sc14b)
	66.063	$2.62^{+0.16}_{-0.16}$	$0.013^{+0.003}_{-0.003}$	⋯	0	PH-3c (Sc14b)
12365184	69.7546	$10.6^{+1.4}_{-1.3}$	$2.5^{+0.3}_{-0.3}$	$1.75^{+0.08}_{-0.07}$	0	Kepler-419b (Da12)
	675.47	n/a	$7.3^{+0.4}_{-0.4}$	⋯	0	Kepler-419c (Da12)
7898352	127.2824031	$9.32^{+3.76}_{-0.77}$	n/a	$0.883^{+0.356}_{-0.073}$	7.2×10^{-2}	Kepler-302c (Ro14)
	30.1836854	$2.88^{+1.15}_{-0.24}$	n/a	⋯	3.4×10^{-5}	Kepler-302b (Ro14)

higher value, but their 90% confidence intervals do not overlap with each other. Even with the extreme case that the HJ companions have a uniform cosine mutual inclination distribution, the 90% confidence interval of its distribution excludes the median of the WJ companion rate distribution. The conclusion holds with a 10% false positive rate (lower panel of Figure 7). If we assume instead a uniform log P distribution for the HJ companions, similar to that of the WJs, the conclusion will be stronger since it allows fewer nontransiting companions.

For interior companions of HJs, we are able to constrain the detection of planets with sizes larger than $1.5\,R_{\rm Earth}$ to be complete up to 10 days. However, this conclusion can be extended to $1\,R_{\rm Earth}$ if we correct for detection completeness assuming that $df/d\log R$ is constant between 1 and $3\,R_{\rm Earth}$ (as suggested by Petigura et al. 2013b). In reality, the majority of

Table 3
Summary of Transiting Companions for *Kepler* Giant Planets

Group	Total	$N_{\rm multi}$	Inner	Outer
HJ	45	0	0	0
Confirmed HJ	28	0	0	0
WJ	27	10	10	3
Confirmed WJ	12	7	7	2

Table 4
The Probability for a Giant Planet to Have at Least One "Close" Companion in the System[a]

Group	Candidate *fp*	Mutual Inclination	HJ Rate (%)	WJ Rate (%)
1	0	0	$0.5^{+5.0}_{-0.5}$	$37.2^{+18.6}_{-16.3}$
2	10%	$\sigma_\mu = 1.^\circ8$	$0.98^{+9.4}_{-0.98}$	$58.1^{+31.7}_{-31.0}$
3	10%	uniform	$8.4^{+46.4}_{-8.0}$	...
4	50%	0	$1.1^{+13.3}_{-1.1}$	$55.7^{+27.0}_{-31.1}$
5	50%	$\sigma_\mu = 1.^\circ8$	$1.6^{+19.5}_{-1.6}$	$69.5^{+24.2}_{-30.8}$
6	50%	uniform	$9.1^{+45.8}_{-8.6}$	...
7	100%	0	$0.8^{+7.7}_{-0.8}$	$58.1^{+23.9}_{-26.9}$

Note.
[a] For cases 1, 4, and 7, a "close" companion refers to those with a period smaller than 50 days. For cases 2, 3, 5, and 6, only the interior companions of the giant planets are considered.

the HJs have orbital periods smaller than 5 days, allowing us to have almost complete detection to 1 $R_{\rm Earth}$ regardless of the size distribution.

The rate of exterior companions is extremely sensitive to the distribution of mutual inclinations; as such, it is difficult to obtain a good constraint. If we assume that every giant planet with an interior companion also has an exterior companion, and that the interior and exterior companions have the same mutual inclination distribution (a Rayleigh distribution with $\sigma_\mu = 1.^\circ8$), the observed number of systems with an exterior companion is expected to be one-quarter of those with interior companions due to the transit probability and detection completeness. This is not in contradiction with the current observations.

3. DISCUSSIONS

Our main results (Figures 6 and 7) that HJs have a companion fraction consistent with zero, while about half of WJs have close neighbors, reveal much about their respective formation mechanisms.

3.1. Two Populations of WJs?

Two previous works have suggested that WJs are not all the same beasts. Using RV data, Dawson & Murray-Clay (2013) suggested that eccentric WJs tend to orbit around metal-rich stars, while planets around metal-poor stars have predominately circular orbits. Later, also based on RV data, Dong et al. (2014) showed that more than half of the eccentric WJs ($e > 0.4$) have distant, Jovian companions, while the low-eccentricity WJs tend to be "single." Taken together, these suggest that more Jovian planets are produced around metal-rich stars, and this somehow raises the eccentricities of WJs (via either secular perturbations or planet–planet scatterings). Recently, Bryan et al. (2016) confirmed the above finding with a larger sample.

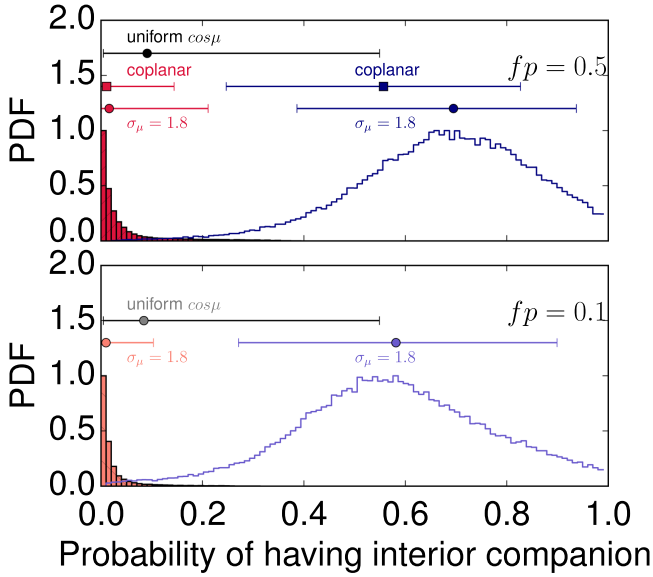

Figure 7. Same as Figure 6, but demonstrating the impact of mutual inclinations, considering only *inner* companions. The top panel compares the *inner* companion rates using our standard priors, with the histograms corresponding to a case where the mutual inclinations are a narrow Rayleigh distribution with a dispersion of $\sigma_\mu = 1.^\circ8$—compare these to the coplanar case. The extreme case, marked with "uniform cosμ" for the HJs only, is one where we assume that the orbital planes for HJs and their inner companions are uncorrelated. The bottom panel shows the same content but for a smaller false positive rate of $fp = 10\%$, a value that we deem more plausible for our sample.

In addition, they reported that WJs have a lower occurance rate of distant giant companions (defined as with masses between 1 and 20 M_J, and at orbital distances of 5–20 AU), compared to what they found regarding the HJs, suggesting that dynamic processes due to giant planetary companians are less important in the WJ systems.

Our study of the *Kepler* transit data adds a further dimension to the picture. At least half of the WJs in our sample are flanked by close, small companions. Most likely, they are nearly coplanar with these companions (to maximize transit probability) and are also nearly circular (to prevent dynamical instability in such closely packed systems). RV counterparts to these objects have been found, e.g., HIP 57274c (Fischer et al. 2012), which is a nearly circular WJ with a small mass neighbor interior to its orbit, GJ 876c (Rivera et al. 2010), and 55 Cnc-b (Endl et al. 2012). However, due to limits on RV precision, most of these WJs will in general be observed as "singles" on largely circular orbits.[5]

How are the WJs formed? For those with low-mass neighbors, we postulate that they are formed in situ, i.e., they undergo runaway gas accretion locally, and that the abundant, closely packed, super-Earth population discovered by *Kepler* consists of the cores enabling the accretion. This hypothesis is supported by the following arguments:

1. Small planets (sub-Jovian) are common around stars, and their frequency rises outward steeply at just the inner edge of our WJ zone (Howard et al. 2012) and remains flat in logarithmic period beyond this cutoff (Petigura et al. 2013a; Silburt et al. 2015).
2. Measured masses for some of these small planets are available (e.g., Weiss et al. 2013; Hadden &

[5] In other words, the transit technique is uniquely capable of revealing these small neighbors.

Lithwick 2014), with some reaching beyond 10 $M_{\rm Earth}$ in solid mass.
3. Such massive cores can retain a heavy enough atmosphere and undergo runaway gas accretion, at the observed locations for these WJs (e.g., Rafikov 2006). Recent theoretical studies of accretion of such an envelope (Lee et al. 2014; Batygin et al. 2015) further argue that cooling can be sufficiently fast to allow in situ formation of giant planets at these distances.
4. As the WJ grows in mass, it can keep the planetary configuration largely intact.[6] As a result, we observe them today still flanked by small neighbors.

Alternative theories such as disk migration, whereby these WJs are formed at larger distances and migrate inward by interaction with the protoplanetary disk, and high-eccentricity migration (such as Kozai migration, planet–planet scattering, etc.) face the challenge of explaining the presence of small neighbors.

What about the other WJs, the ones that have no transiting companions? Studies mentioned above argue that these may be a distinct population. However, it needs to be firmly established that these WJs indeed always have distant Jovian companions, and/or are largely eccentric, and/or only reside around metal-rich stars. At the moment, their origin remains an enigma.

Assuming that the lonely WJs in our sample are from a distinct population, we can estimate the relative proportions of these two groups of WJs. Among the WJs, 10 out of 27 are in multiple systems, or 37^{+19}_{-16}% of WJs. However, this value can rise to 58^{+31}_{-31}% if the mutual inclination dispersion of the system follows a Rayleigh distribution peaked at $1\overset{\circ}{.}8$. In other words, at least half of all WJs are formed in situ.

3.2. Formation of HJs

We were initially motivated by the discovery of close companions around the HJ WASP-47b (Becker et al. 2015). After having established the general patten among hot and WJs, we return to reflect on the existence of this particular system.

WASP-47b was first identified by ground-based photometry and then verified with RV measurements (Hellier et al. 2012). Thanks to this detection, it was proposed as a target for the K2 mission. In the meantime, the radial-velocity monitoring of the system unveiled a second, long-period gas giant (Neveu-VanMalle et al. 2016). Becker et al. (2015) analyzed the K2 data and announced the presence of two super-Earths, one inner to the HJ and one between both gas giants. The two low-mass companions of WASP-47b were discovered in a targeted observation, so it is difficult to ascertain their statistical importance. However, we can set an upper limit on the frequency of such objects, based on the absence of neighbors in our HJ sample. This is $1.0^{+9.5}_{-1.0}$% among all HJs, assuming a candidate false positive rate of 10% and a mutual inclination dispersion of $1\overset{\circ}{.}8$ (Table 2).

This leads us to believe that WASP-47b is a rather unique system among HJs, themselves rare systems. Based on our discussion above, we further speculate that since more than half of WJs may be formed in situ, this path may find its way into the period domain of HJs. Or, WASP-47b is also formed in situ (Batygin et al. 2015; Boley et al. 2016) and is a tail of the in situ WJs. Given the relative numbers of HJs (one, WASP-47b) and WJs (7 out of the confirmed sample of 12) in multiple systems and the lower transit probability of WJs, this would suggest that the in situ process is increasingly difficult for closer-in planets, with WASP-47b being the hottest representative of the WJ population.

Where do the majority of the HJs come from then? We turn to the observations for the answer. Many of the dynamical migration processes that are invoked to explain HJs invariably produce the so-called 3-day pileup, an excess of HJs near the 3-day orbital period. Such a pileup, originally discovered among the RV population (Wright et al. 2009), but then found to be absent in the *Kepler* transit data (Howard et al. 2012), and then rediscovered recently through careful RV falsification of the transit candidates (Santerne et al. 2016), now seems here to stay. The HJs that went through dynamical migration also naturally led to the destructions of any inner planets in the system (Mustill et al. 2015). This lends support to the hypothesis that HJs are products of violent dynamical processes.

4. CONCLUDING WORDS

When we set out on this project, we wondered whether WASP-47b is a commonplace HJ in terms of small neighbors. By examining the *Kepler* HJs, we found that systems such as WASP-47b are rare among the HJs—among our statistical sample of 45 (28 confirmed) HJs, none show small companions, either inner or outer.

In contrast, we found that among our WJ sample, half or more have nearly coplanar, small companions. Most of these are inner companions, and given the fact that exterior companions are less likely to transit, the data give the impression that they are at least as common as the inner ones (Table 1).

So not only do HJs and WJs appear to be separated in their period distributions (Santerne et al. 2016), but they are also distinct in their respective fractions of close neighbors.

Motivated by this discovery and by recent theoretical progress in understanding gas accretion, we propose that a significant fraction of WJs are formed in situ. The prevalence of multiple low-mass planets in close proximity to one another and to the star can, in a fraction of the cases, permit some of the planets to accrete enough envelope and to trigger runaway growth. This process can operate in the WJ locale, but appears to become increasingly difficult toward the HJ region, explaining the rarity of systems like WASP-47b.

We outline future directions below:

1. The true neighbor fractions of WJs are sensitive to the inclination dispersion in the system, as well as the false positive rate of our WJ sample (Table 2). Both could be improved. Specifically, further photometric and RV monitoring of the confirmed WJs discovered by ground-based transit surveys, such as HAT-P-15b (Kovács et al. 2010) and HATS-17b (Brahm et al. 2016), are likely to reveal the presence of companions, if current statistics hold.
2. Masses for these close companions are interesting. They may yield the critical mass above which runaway gas accretion occurs.
3. Multiple lines of evidence suggest that there may be a second population of WJs. But data are inconclusive at

[6] It will be able to destabilize some of the closest neighbors and ingest them in the process.

the moment. Studies of WJ eccentricity distribution, host star metallicity distribution, the presence of giant-planet companions, etc., may help answer whether there is a second pathway to form WJs.
4. The in situ WJs accrete their gas inward of the ice line. As such, their envelope water content should not be depleted by condensation. This may contrast with those that accrete their gas beyond the ice line (barring core erosion in these bodies) and may be testable by transmission spectroscopy.
5. Using transit data, we can exclude inner neighbors of HJs, but the constraint is less stringent for the outer neighbors, especially if they may be highly misaligned (Batygin et al. 2015). RV studies are necessary.
6. If outer neighbors are indeed also absent among HJs, theoretical study is needed to explain the rarity of in situ formation for HJs, versus that of WJs.

The Dunlap Institute is funded through an endowment established by the David Dunlap family and the University of Toronto. References to exoplanetary systems were obtained through the use of the paper repositories, ADS and arXiv, but also through frequent visits to the exoplanet.eu (Schneider 2011) and exoplanets.org (Wright et al. 2011) websites. This paper includes data collected by the *Kepler* mission. Funding for the *Kepler* mission is provided by the NASA Science Mission directorate. Some of the data presented in this paper were obtained from the Multimission Archive at the Space Telescope Science Institute (MAST). STScI is operated by the Association of Universities for Research in Astronomy, Inc., under NASA contract NAS5-26555. Support for MAST for non-*HST* data is provided by the NASA Office of Space Science via grant NNX09AF08G and by other grants and contracts. This research has made use of the NASA Exoplanet Archive, which is operated by the California Institute of Technology, under contract with the National Aeronautics and Space Administration under the Exoplanet Exploration Program.

APPENDIX
STATISTICAL FRAMEWORK

The observed giant-planet multiplicity systems $N_{\rm obs,m}$ can arise from four origins: the confirmed multiple-planet systems $N_{\rm obs,p,m}$, candidate multiple-planet systems $N_{\rm obs,gc,m}$ with at least a giant planet, candidate multiple-planet systems with the most massive planet being Neptune nature $N_{\rm obs,nc,m}$, and false positive multiple systems due to binary contamination $N_{\rm obs,s,m}$. We assume the contribution to the multiple system with a giant planet from false positives ($N_{\rm obs,s,m}$) to be negligible (Lissauer et al. 2014):

$$N_{\rm obs,m} = N_{\rm obs,p,m} + N_{\rm obs,gc,m} + N_{\rm obs,nc,m}. \quad (2)$$

The individual terms above can be expressed as follows:

$$N_{\rm obs,p,m} = N_{\rm p} f(g, m) f(d), \quad (3)$$

where $N_{\rm p}$ is the total number of confirmed systems we have, $f(g, m)$ is the rate of giant-planet systems having a close-in companion, and $f(d)$ is the probability for this companion to be detected.

The number of multiple systems that originated from "Jupiters" and "Neptunes" can be estimated as

$$N_{\rm obs,gc,m} = N_{\rm pc} f(g) f(g, m) f(d) \quad (4)$$

and

$$N_{\rm obs,nc,m} = N_{\rm pc}(1 - f(g)) f(n, m) f(d), \quad (5)$$

where $f(g)$ is the fraction of giant planets in the our selected radius range, and $f(g, m)$ and $f(n, m)$ are the probabilities of a Jupiter/Neptune-size planet having a close-in companion. $N_{\rm pc}$ is the number of planetary candidates that have planet nature,

$$N_{\rm pc} = (N - N_{\rm p}) \times (1 - fp), \quad (6)$$

with fp denoting the false positive rate of an unconfirmed KOI.

The problem can be summarized as a Bayesian problem, in which N_m is observable, and $f(g, m)$, $f(n, m)$, $f(FP)$, and $f(g)$ as parameters we want to constrain given the data. We can do this by sampling the posterior space:

$$p(\hat{f}|w\hat{}_{\rm obs}) = p(\hat{f}) \times p(w\hat{}_{\rm obs}|\hat{f}). \quad (7)$$

The likelihood $p(w\hat{}_{\rm obs}|\hat{f})$ can be expressed as $B(N_{\rm obs,m} - N_{\rm obs,nc,m}|f(g, m), N_p + N_{\rm pc,g})$, in which $B(s|x, N)$ indicate the probability of observing s success given N observations with success rate x.

The priors $p(\hat{f})$ are assumed (estimated) as below.

1. We use a conjugate prior for the multiplicity rate of a giant planet $f(g, m)$.
2. $f(g)$ is the probability of an unconfirmed planet to be a giant planet. We use the posterior of the radius distribution of the candidate to decide the probability of a candidate to have a radius smaller than $8\,R_{\rm Earth}$. We derived the average probability of an unconfirmed HJ to be a Neptune to be Beta(2.06, 15.9), and for a WJ to be Beta(2.65, 18.4).
3. We use the multiplicity rate for the super-Neptunes ($4\,R_{\rm Earth} < R_p < 8\,R_{\rm Earth}$) within our designed stellar parameter and period range, in the entire KOI sample (25 out of 140), as a prior for $f(n, m)$. We note that this rate is quite uncertain; Mayor et al. (2011) report that the multiplicity rates for small planets are ~70% with an unclear statistic significance. Given that the rate of $f(g)$ is small, the choice of $f(g)$ does not impact the final result significantly.
4. We use two sets of false positive rates. We first use the false positive rate from Santerne et al. (2016) to estimate the false positive rate of an unconfirmed candidate fp. Santerne et al. (2016) identified 46 false positives out of 100 KOIs in the effective temperature and period range we use. For HJs, the FP rate is 42.8%, and 49% for WJs. This is lower than the overall false positive rate reported by Santerne et al. (2016), since the authors found that the false positive rate around stars with $T_{\rm eff}$ higher than 6500 K is generally higher, which are not included in our sample. We apply a beta distribution prior for the false positive rate. Due to our additional selection on our candidates, the actual false positive rate can be even lower. We use the astrophysical false positive rate estimated by Morton et al. (2016, in preparation) to obtain a more optimistic value (10%).
5. We do not attempt to factor in the actual value of the detection completeness $f(d)$ for our estimation of the final

rate since the size distributions of small planets have big uncertainties. We note that the detection is complete to $2\,R_{\rm Earth}$ with orbital period less than 50 days for both HJs and WJs. For interior companions, it is complete for HJs to $1.5\,R_{\rm Earth}$. We are able to prove that our conclusions are not changed if we extend this size limit to $1\,R_{\rm Earth}$ by assuming that $df/d\log R$ is constant between 1 and $3\,R_{\rm Earth}$ as suggested by Petigura et al. (2013b). Our experiment found that counting smaller planets is equivalent to assuming a more dispersed mutual inclination distribution for both HJs and WJs. Unless the occurrence rate of planets has a steep rise toward small size, it does not impact the companion rate of HJs much, while the companion rate of WJs may shift to a higher value.

To take into account the effect of mutual inclination angle dispersion, we compute an averaged transit probability for HJs and WJs separately on a mutual inclination grid with $\cos\mu$ from 0 to 1. We later interpolate on this grid to obtain the transit probability at an arbitrary mutual inclination angle in our simulations. Since the inclination angle of the giant planet i_g is usually loosely constrained by the transit fit, we assume that $\cos i_g$ has a uniform probability as long as the planet transit. We also integrate over the possible period range the companion could take:

$$\bar{f}_{\rm tran}(\mu) = \frac{1}{N}\int f_{\rm tran}(\text{period}, i_g, \mu) P(\text{period}) P(i_g)\, d\text{period}\, di_g \tag{8}$$

For the probability of the companion occuring at a certain orbital period, we use the formalism from Howard et al. (2012) for the HJs:

$$df/d\,\log(\text{period}) \propto \text{period}^{\beta}(1 - e^{-(\text{period}/7.0\text{day})^{\gamma}}), \tag{9}$$

where $\beta = 0.27 \pm 0.27$ and $\gamma = 2.6 \pm 0.3$. For period < 10 days, this can be approximated with $f(\text{period}) \propto \text{period}^2$. We use the latter in our calculation. For WJs, we assume $df/d\log(\text{period}) = C$ instead with a cutoff inner period at 1 day.

The likelihood expression can be revised as $B(N_m|f(g, m)f_{\rm tran}, N_p + N_{\rm pc,g})$ as a conditional binomial problem. Here we are assuming that the covariance between $f(g, m)$ and $f_{\rm tran}$ is 0.

We choose two types of priors for the mutual inclination of HJs, a Rayleigh distribution with $\sigma_\mu = 1.8$, and a uniform distribution for $\cos\mu$ between 0 and 1. We only use the Rayleigh distribution prior for the WJs.

REFERENCES

Almenara, J. M., Damiani, C., Bouchy, F., et al. 2015, A&A, 575, A71
Batygin, K., Bodenheimer, P. H., & Laughlin, G. P. 2015, arXiv:1511.09157
Becker, J. C., Vanderburg, A., Adams, F. C., Rappaport, S. A., & Schwengeler, H. M. 2015, ApJL, 812, L18
Boley, A. C., Granados Contreras, A. P., & Gladman, B. 2016, ApJL, 817, L17
Bonomo, A. S., Hébrard, G., Santerne, A., et al. 2012, A&A, 538, A96
Bonomo, A. S., Sozzetti, A., Santerne, A., et al. 2015, A&A, 575, A85
Borucki, W. J., Koch, D. G., Basri, G., et al. 2011, ApJ, 736, 19
Brahm, R., Jordán, A., Bakos, G. Á, et al. 2016, AJ, 151, 89
Bruno, G., Almenara, J.-M., Barros, S. C. C., et al. 2015, EPJWC, 101, 06014
Bryan, M. L., Knutson, H. A., Howard, A. W., et al. 2016, ApJ, 821, 89
Buchhave, L. A., Latham, D. W., Carter, J. A., et al. 2011, ApJS, 197, 3
Cabrera, J., Csizmadia, S., Lehmann, H., et al. 2014, ApJ, 781, 18
Dawson, R. I., Johnson, J. A., Morton, T. D., et al. 2012, ApJ, 761, 163
Dawson, R. I., & Murray-Clay, R. A. 2013, ApJL, 767, L24
Dawson, R. I., Murray-Clay, R. A., & Johnson, J. A. 2015, ApJ, 798, 66
Deleuil, M., Almenara, J.-M., Santerne, A., et al. 2014, A&A, 564, A56
Dong, S., Katz, B., & Socrates, A. 2014, ApJL, 781, L5
Dong, S., & Zhu, Z. 2013, ApJ, 778, 53
Endl, M., Caldwell, D. A., Barclay, T., et al. 2014, ApJ, 795, 151
Endl, M., MacQueen, P. J., Cochran, W. D., et al. 2011, ApJS, 197, 13
Endl, M., Robertson, P., Cochran, W. D., et al. 2012, ApJ, 759, 19
Esteves, L. J., De Mooij, E. J. W., & Jayawardhana, R. 2015, ApJ, 804, 150
Fabrycky, D. C., Lissauer, J. J., Ragozzine, D., et al. 2014, ApJ, 790, 146
Faigler, S., Tal-Or, L., Mazeh, T., Latham, D. W., & Buchhave, L. A. 2013, ApJ, 771, 26
Fang, J., & Margot, J.-L. 2012, ApJ, 761, 92
Figueira, P., Marmier, M., Boué, G., et al. 2012, A&A, 541, A139
Fischer, D. A., Gaidos, E., Howard, A. W., et al. 2012, ApJ, 745, 21
Foreman-Mackey, D., Hogg, D. W., Lang, D., & Goodman, J. 2013, PASP, 125, 306
Fressin, F., Torres, G., Charbonneau, D., et al. 2013, ApJ, 766, 81
Gandolfi, D., Parviainen, H., Fridlund, M., et al. 2013, A&A, 557, A74
Gibson, N. P., Pollacco, D., Simpson, E. K., et al. 2009, ApJ, 700, 1078
Hadden, S., & Lithwick, Y. 2014, ApJ, 787, 80
Hébrard, G., Santerne, A., Montagnier, G., et al. 2014, A&A, 572, A93
Hellier, C., Anderson, D. R., Collier Cameron, A., et al. 2012, MNRAS, 426, 739
Howard, A. W., Marcy, G. W., Bryson, S. T., et al. 2012, ApJS, 201, 15
Huang, X., Bakos, G. Á, & Hartman, J. D. 2013, MNRAS, 429, 2001
Jenkins, J. M., Borucki, W. J., Koch, D. G., et al. 2010, ApJ, 724, 1108
Koch, D. G., Borucki, W. J., Rowe, J. F., et al. 2010, ApJL, 713, L131
Kovács, G., Bakos, G. Á, Hartman, J. D., et al. 2010, ApJ, 724, 866
Latham, D. W., Borucki, W. J., Koch, D. G., et al. 2010, ApJL, 713, L140
Latham, D. W., Rowe, J. F., Quinn, S. N., et al. 2011, ApJL, 732, L24
Lee, E. J., Chiang, E., & Ormel, C. W. 2014, ApJ, 797, 95
Lillo-Box, J., Barrado, D., & Bouy, H. 2014, A&A, 566, A103
Lissauer, J. J., Marcy, G. W., Bryson, S. T., et al. 2014, ApJ, 784, 44
Lissauer, J. J., Ragozzine, D., Fabrycky, D. C., et al. 2011, ApJS, 197, 8
Lithwick, Y., Xie, J., & Wu, Y. 2012, ApJ, 761, 122
Mayor, M., Marmier, M., Lovis, C., et al. 2011, arXiv:1109.2497
Morton, T. D. 2012, ApJ, 761, 6
Morton, T. D., Bryson, S. T., Coughlin, J. L., et al. 2016, ApJ, 822, 86
Mustill, A. J., Davies, M. B., & Johansen, A. 2015, ApJ, 808, 14
Nesvorný, D., Kipping, D. M., Buchhave, L. A., et al. 2012, Sci, 336, 1133
Neveu-VanMalle, M., Queloz, D., Anderson, D. R., et al. 2016, A&A, 586, A93
O'Donovan, F. T., Charbonneau, D., Mandushev, G., et al. 2006, ApJL, 651, L61
Ofir, A., & Dreizler, S. 2013, A&A, 555, A58
Pál, A., Bakos, G. Á, Torres, G., et al. 2008, ApJ, 680, 1450
Petigura, E. A., Howard, A. W., & Marcy, G. W. 2013a, PNAS, 110, 19273
Petigura, E. A., Marcy, G. W., & Howard, A. W. 2013b, ApJ, 770, 69
Rafikov, R. R. 2006, ApJ, 648, 666
Rivera, E. J., Laughlin, G., Butler, R. P., et al. 2010, ApJ, 719, 890
Rowe, J. F., Bryson, S. T., Marcy, G. W., et al. 2014, ApJ, 784, 45
Sanchis-Ojeda, R., Fabrycky, D. C., Winn, J. N., et al. 2012, Natur, 487, 449
Santerne, A., Díaz, R. F., Moutou, C., et al. 2012, A&A, 545, A76
Santerne, A., Moutou, C., Tsantaki, M., et al. 2016, A&A, 587, A64
Schmitt, J. R., Agol, E., Deck, K. M., et al. 2014a, ApJ, 795, 167
Schmitt, J. R., Wang, J., Fischer, D. A., et al. 2014b, AJ, 148, 28
Schneider, J. 2011, in EPSC-DPS Joint Meeting, 3
Seager, S., & Mallén-Ornelas, G. 2003, ApJ, 585, 1038
Shporer, A., Jenkins, J. M., Rowe, J. F., et al. 2011, AJ, 142, 195
Silburt, A., Gaidos, E., & Wu, Y. 2015, ApJ, 799, 180
Southworth, J. 2011, MNRAS, 417, 2166
Steffen, J. H., & Agol, E. 2005, MNRAS, 364, L96
Steffen, J. H., Batalha, N. M., Borucki, W. J., et al. 2010, ApJ, 725, 1226
Steffen, J. H., Ragozzine, D., Fabrycky, D. C., et al. 2012, PNAS, 109, 7982
Tremaine, S., & Dong, S. 2012, AJ, 143, 94
Van Eylen, V., Kjeldsen, H., Christensen-Dalsgaard, J., & Aerts, C. 2012, AN, 333, 1088
Wang, J., Fischer, D. A., Barclay, T., et al. 2013, ApJ, 776, 10
Weiss, L. M., Marcy, G. W., Rowe, J. F., et al. 2013, ApJ, 768, 14
Wright, J. T., Fakhouri, O., Marcy, G. W., et al. 2011, PASP, 123, 412
Wright, J. T., Marcy, G. W., Howard, A. W., et al. 2012, ApJ, 753, 160
Wright, J. T., Upadhyay, S., Marcy, G. W., et al. 2009, ApJ, 693, 1084
Xie, J.-W. 2013, ApJS, 208, 22